ELSEVIER

Chemical Physics 226 (1998) 83–99

Chemical Physics

Effect of substituents on the spectroscopic properties of all-*trans*-1,6-diphenyl-1,3,5-hexatriene

G. Pistolis, Angelos Malliaris *

NRC 'Demokritos', Athens 153 10, Greece

Received 14 July 1997

Abstract

An extensive spectroscopic study of two derivatives of the all-*trans*-1,6-diphenyl-1,3,5-hexatriene (DPH) has been conducted. The one derivative carries, at the *para* position of one of the phenyl rings of the parent molecule, the electron donating $-N-(CH_3)_2$ group, while the other carries at the same position the electron withdrawing $-NO_2$ substituent. The absorption–fluorescence spectra, quantum yields, lifetimes and steady state fluorescence anisotropies of these derivatives, were studied in various solvents, at different temperatures and at different viscosities. The findings are presented and discussed along with the exceptional fluorescence probing properties of these two particular derivatives. For comparative purposes, the main spectroscopic properties of the parent molecule are also included. © 1998 Elsevier Science B.V.

1. Introduction

Historically, polyenes $(-CH=CH-)_n$ were one of the first examples of organic molecules for which approximate quantum mechanical calculations, viz. the free-electron model, were developed aiming at the determination of their molecular electronic energy levels [1]. These molecules and their derivatives have been the subject of intense research for many years because of their relation to important biological structures, e.g., vitamin A1, carotenoids, the crucial for the visual cycle in rod cells 11-*cis*-retinal, etc. Another important aspect of these molecules is the *cis–trans* photoisomerization occurring in polyenes and their derivatives [2]. Polyenes and their derivatives present special interest also from the purely spectroscopic point of view. Thus, the all-*trans*-1,6-diphenyl-1,3,5-hexatriene (DPH), has been extensively studied because it is a typical homologue of this series which exhibits dual fluorescence originating from two different excited states, viz. $^1A_g(S_1)$ and $^1B_u(S_2)$, at thermal equilibrium [3–5]. Regarding chemical and biological applications DPH has also found wide use because of its fluorescence anisotropy, which in conjunction with its fluorescence lifetime, renders this molecule indispensable for local fluidity studies in microcompartmentalized and supramolecular systems [6]. Because of their probing capabilities, which they share with the parent molecule, several DPH derivatives have been synthesized and used as fluorescent probes, these include neutral molecules, e.g., NO_2–DPH–NO_2 [7,8], anions, e.g., DPH–$(CH_2)_2COO^-$ [9], cations, e.g., DPH–$N(CH_3)_3^+$ [10], surfactants, e.g., DPH-containing phosphatidylcholine [11], etc. However, complete and detailed spectroscopic data have not been published for any of these DPH derivatives,

* Corresponding author.

0301-0104/98/$19.00 © 1998 Elsevier Science B.V. All rights reserved.
PII S0301-0104(97)00302-9

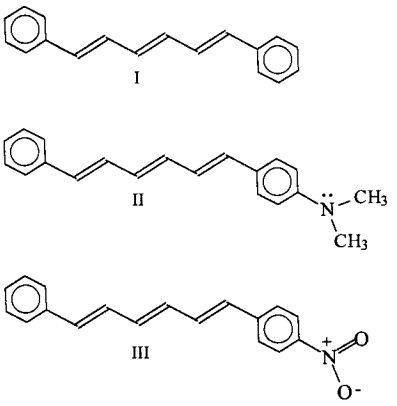

Scheme 1.

only scattered and uncorrelated results have occasionally appeared in the literature [7,8,12,13].

In the present work, we have undertaken an extensive spectroscopic study of two neutral DPH derivatives, namely 1-(4′-dimethylammoniumphenyl)-6-phenyl-1,3,5-hexatriene (II), and 1-(4′-nitrophenyl)-6-phenyl-1,3,5-hexatriene (III), (see Scheme 1). These molecules were chosen as subject of the present study mainly for two reasons. Firstly, because they contain two characteristic substituents, a typical electron donor, $-N(CH_3)_2$, and a typical electron acceptor, $-NO_2$. The attachment of such substituents is expected to affect the charge delocalization in the extended conjugated system of DPH leading to important solute–solvent interactions, and sizable spectral shifts. Therefore spectroscopic findings concerning II and III are also relevant to other DPH derivatives. The second reason is that these two particular molecules have been shown to demonstrate exceptional sensitivity to the micropolarity as well as to the microviscosity of their environment [14]. Indeed, derivatives II and III are more versatile fluorescent probes than DPH itself, since they are capable of simultaneously probing microfluidity (through their fluorescence anisotropy), and micropolarity (by means of their solvent sensitive fluorescence red shift) of the same microenvironment under identical conditions. Note, that the parent molecule DPH cannot probe micropolarity in liquid solutions because of its peculiar spectroscopic behaviour which arises from the fact that the electronic transition $^1A_g(S_0) \leftarrow {}^1A_g(S_1)$, responsible for practically all fluorescence intensity, is symmetry forbidden in the C_{2h} point group of diphenyl-*n*-polyenes [15]. A consequence of the forbidden character of the fluorescence transition, is that this transition is insensitive to solvent polarity. For this reason DPH cannot probe the polarity of its liquid environment. The obvious way to improve the sensitivity of the fluorescence of DPH to environmental changes would be to lower its point group symmetry and make allowed the symmetry forbidden transitions. Indeed, in II and III the lack of an inversion centre (point group symmetry C_s) makes allowed all the symmetry forbidden transitions of the type $g \rightarrow g$, or $u \rightarrow u$, responsible for the 'anomalous' electronic spectra of polyenes and diphenylpolyenes. Finally, it should be mentioned that the sole spectroscopic information published about the amino [10] and nitro [7,8] derivatives of DPH amounting to only few absorption–emission spectra, and some fluorescence quantum yields and lifetimes, are discussed here and compared to our own findings.

2. Experimental

The parent molecule, all-*trans*-1,6-diphenyl-1,3,5-hexatriene (DPH) was purchased from Fluka, while its two derivatives, viz. 1-(4′-dimethylaminophenyl)-6-phenyl-1,3,5-hexatriene (abbr. DPH–$N(CH_3)_2$) and 1-(4′-nitrophenyl)-6-phenyl-1,3,5-hexatriene (abbr. DPH–NO_2) were from Lambda Probes and Diagnostics. All three compounds were of the highest purity available and therefore were used without further purification, however, their high purity, as well as that of the solvents used, was confirmed by absorption and fluorescence spectroscopy. Also because of the low solubility of these molecules in some solvents, we have confirmed the formation of proper solutions by verifying, in all cases, the validity of Beer's law. For absorption spectra the Perkin–Elmer Lambda-16 spectrophotometer was employed. Fluorescence and excitation spectra were recorded on a Perkin–Elmer LS50-B fluorometer equipped with filter polarizers. The same instrument was used to determine the fluorescence anisotropy, r. The excitation wavelength used for the determination of the fluorescence anisotropy was 356 nm for DPH, 390 nm for DPH–

$N(CH_3)_2$, and 405 nm for DPH–NO_2. The concentrations employed for all measurements, except absorption, were 5×10^{-7} M for DPH and 10^{-6} M for the two derivatives. All emission spectra reported here were corrected for the response of the instrument. Fluorescence quantum yields (Φ_f) were obtained from deoxygenated solutions, employing as standard a solution of quinine sulfate in 1.0 M sulfuric acid for which $\Phi_f^{st} = 0.55$ [16], and using the equation

$$\Phi_f = \Phi_f^{st} \frac{F}{F^{st}} \frac{OD^{st}}{OD} \left(\frac{n_D}{n_D^{st}} \right)^2 .$$

In this equation F and F^{st} stand for the integrated fluorescence spectra, OD and OD^{st} are the optical densities at the wavelength of excitation and n_D and n_D^{st} are the refractive indices, all symbols referring to the solution under study and the standard quinine sulfate solution, respectively. The temperature range of our measurements extends from 300 down to 77 K. Fluorescence lifetimes τ(exp), were determined using the time correlated single photon counter FL900 of Edinburgh Instruments. The calculated intrinsic lifetimes of the excited state, τ(intr), were estimated from the absorption spectra using the formula [17]

$$\frac{1}{\tau_{intr}} = 2.88 \times 10^{-9} n_D^2 \langle \bar{\nu}_f^{-3} \rangle_{av.}^{-1} \int \frac{\epsilon(\bar{\nu}) d\bar{\nu}}{\bar{\nu}} \quad (1)$$

where $\langle \bar{\nu}_f^{-3} \rangle_{av.}^{-1}$ is the reciprocal of the mean value of $\bar{\nu}^{-3}$ in the fluorescence spectrum.

$$\langle \bar{\nu}_f^{-3} \rangle_{av.}^{-1} = \frac{\int F(\bar{\nu}) d\bar{\nu}}{\int F(\bar{\nu}) \bar{\nu}^{-3} d\bar{\nu}} \quad (2)$$

whereas $\int \epsilon(\bar{\nu}) d\bar{\nu}/\bar{\nu}$ stands for the integrated intensity, of the absorption coefficient, ϵ, divided by the wavenumber, over the entire range of absorption, the other symbols have the same meanings as in the previous equation of the quantum yield. Refractive indices n_D, when not available from tables, were measured using a thermostated Abbe type refractometer.

3. Results and discussion

When the *para*-H in one of the phenyl rings of DPH is replaced by a substituent the symmetry of the parent molecule is lowered, and therefore the derivatives are expected to exhibit different spectroscopic behaviour from that of DPH. Moreover, the presence of the substituents will modify the energies of the electronic states of the conjugated double bond system, through resonance and inductive interactions. Further differentiation, particularly with respect to the solute–solvent interactions, arises from the fact that contrary to DPH, the two derivatives posses ground state dipole moment, which leads to energy stabilization, – more so in the excited state – and therefore increased red shifts. In order to emphasize the differences in the spectral behaviour of DPH caused by the substitution, we have studied, along with the two derivatives, the parent molecule as well, although its spectroscopy has been extensively discussed in the literature [18]. Our results for DPH were found in very good agreement with those published.

Figs. 1 and 2 show the absorption and fluorescence spectra of DPH, DPH–$N(CH_3)_2$ and DPH–NO_2 in solvents classified according to their refractive indices n_D, and dielectric constants ϵ. Thus, the solvents of Fig. 1a, hexane and benzene, have low and similar ϵ (1.88; 2.28), but very different n_D (1.372; 1.498); in Fig. 1b, the solvents DMF and *p*-dioxane, have high and similar n_D (1.427; 1.422) but different ϵ (36.7; 2.21); in Fig. 2a, ethylether and acetonitrile, have similar and low n_D (1.352; 1.342) with different ϵ values (4.33; 36.2) and in Fig. 2b, acetonitrile and DMF, have high and similar ϵ (36.2; 36.7) and different n_D (1.342; 1.427). Note, that the solvents of Figs. 1 and 2 do not have any tendency for specific interactions with the solutes, e.g., hydrogen bonding, complex formation, electron transfer etc, only effects due to n_D and ϵ, the so-called universal solvent effects, influence the spectra.

3.1. Absorption

Inspection of Figs. 1 and 2 discloses several interesting points concerning the absorption spectra of these molecules. The two derivatives have in all solvents spectra which are red-shifted, up to ca. 3000 cm^{-1}, with respect to the corresponding absorption of the parent molecule DPH, (compare, e.g., DPH

and DPH–NO_2 in hexane). This is the red shift arising from the effect of the substitution of groups such as N–$(CH_3)_2$ and –NO_2, in molecules with extended conjugation. Indeed, the diamino derivative is expected to demonstrate sizable spectral shift with respect to DPH, because the lone electron pair on the N atom can be easily delocalized in the extended conjugated system of the diphenylhexatriene framework. Nitro groups, on the other hand, are known to have nearly the strongest resonance effects of all substituents, on conjugated systems, and this can explain the larger red shifts observed in the absorption spectra of DPH–NO_2. Note that the n → π^* transitions, expected to appear at the low energy part of the absorption spectra, are not observed, evidently because such weak transitions are buried underneath the much stronger $\pi \rightarrow \pi^*$ transitions. Regarding the effect of the environment on the absorption spectra, it is clear from Figs. 1 and 2 that the refractive index n_D of the solvent appears to be, as expected, the determining factor for the red shifts observed in all three homologues. Thus, when the spectra of DPH are compared in hexane and in benzene, i.e., two solvents with very different refractive indices but very similar and low valued dielectric constants, the shift is more than 600 cm^{-1}, as

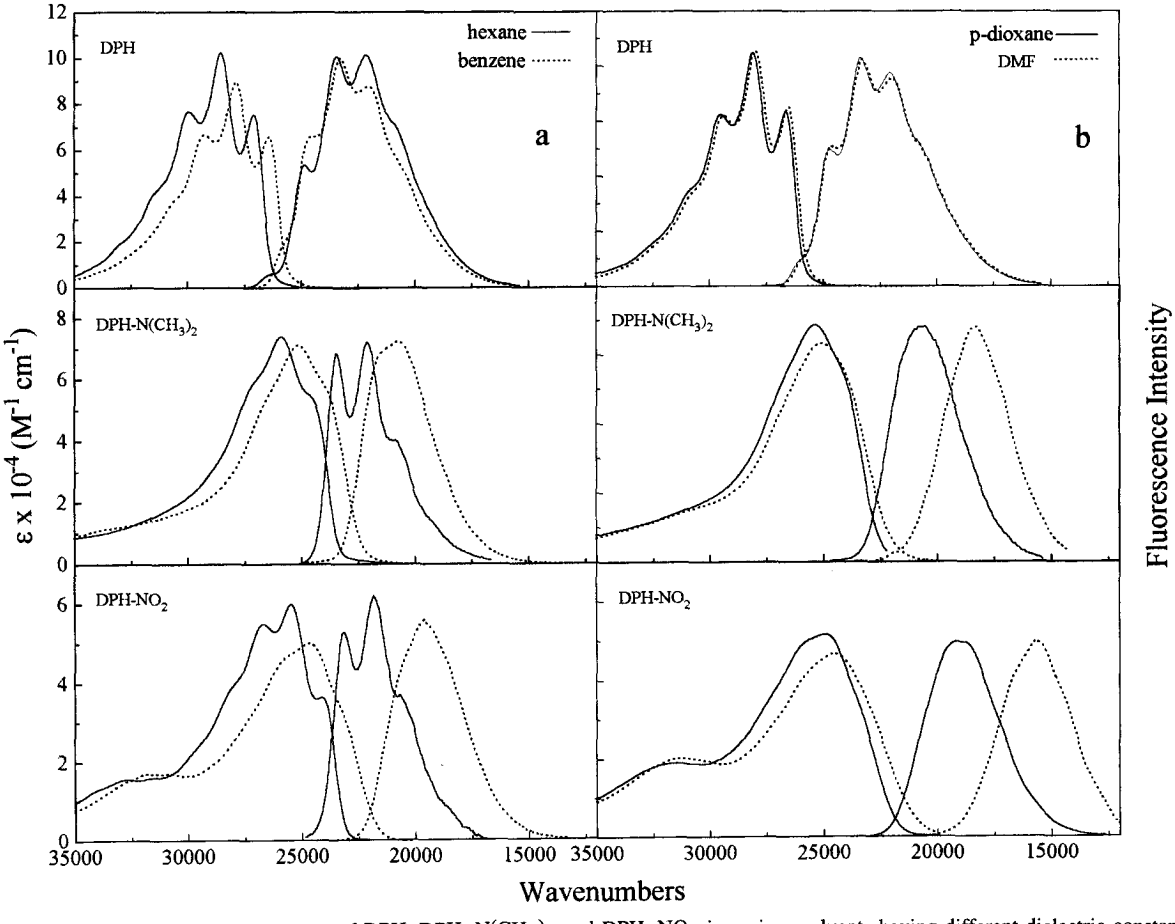

Fig. 1. Absorption–fluorescence spectra of DPH, DPH–$N(CH_3)_2$ and DPH–NO_2 in various solvents having different dielectric constants and refractive indices, as indicated on the panels.

shown in Fig. 1a. Similarly the corresponding shifts, between hexane and benzene, of the polar derivatives DPH–N$(CH_3)_2$ and DPH–NO_2, is ca. 800 cm^{-1}, (see Fig. 1a). The same conclusions are drawn by comparing the spectra of Fig. 2b, where the solvents, acetonitrile and DMF, have again different refractive indices and nearly identical but high valued dielectric constants. Note, also that in Fig. 1a the red shifts are more than the corresponding ones in Fig. 2b, this is because in the former case the difference in n_D between the two solvents, hexane and benzene, is larger than in the latter case.

To further investigate the effect of the refractive index on the absorption spectra we have used hexane–benzene mixed solvents in which, while ϵ remains practically unchanged, between 1.88 and 2.28, n_D changes greatly from 1.372 in pure hexane to 1.498 in pure benzene. The results, shown in Fig. 3 follow the trend expected from theories treating the solute–solvent interactions. These interactions are complex and most theoretical approaches take into account only polarization forces, i.e., the treatments concern cases of non-polar solutes in non-polar solvents [19]. In such an approximate theory [20–22], based on the assumption that the solvent can be described by a continuum cavity model of the On-

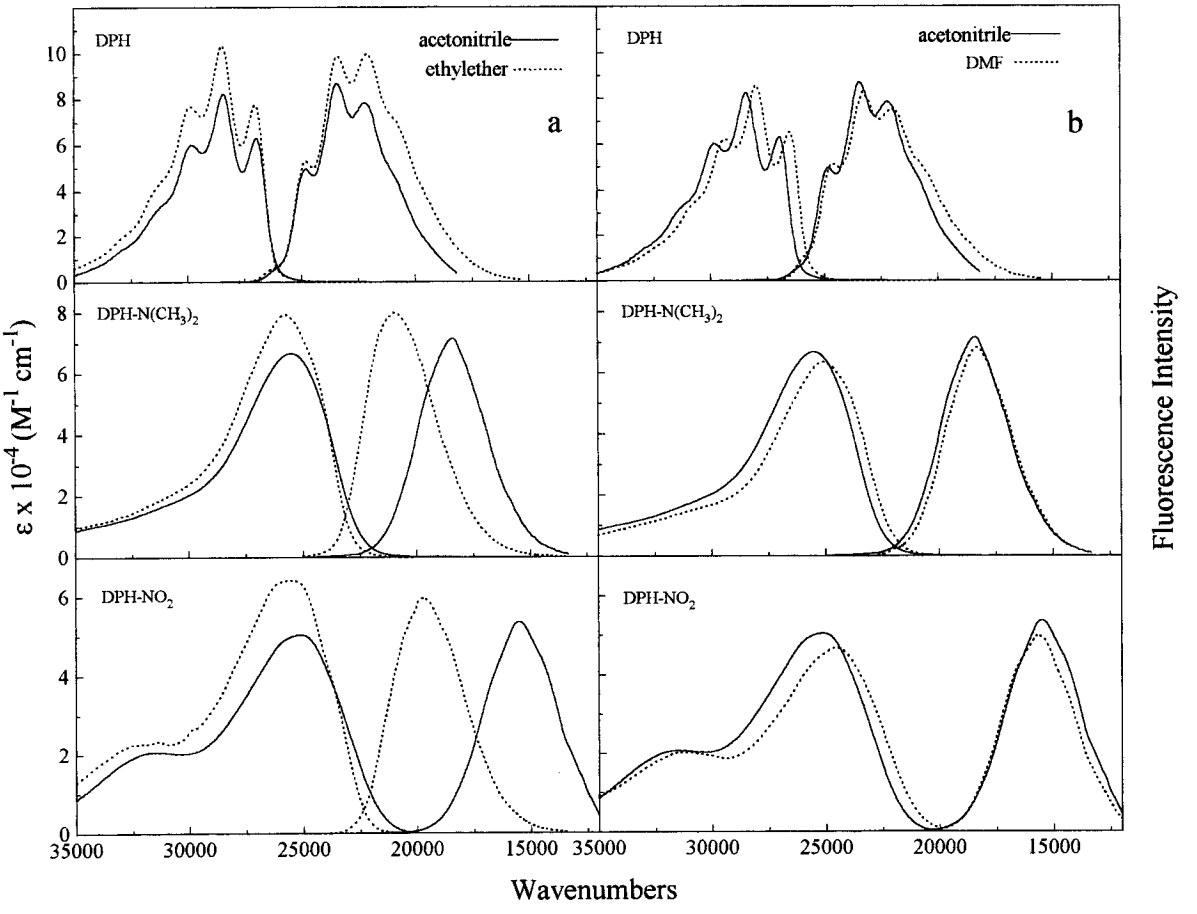

Fig. 2. Absorption–fluorescence spectra of DPH, DPH–N$(CH_3)_2$ and DPH–NO_2 in various solvents having different dielectric constants and refractive indices, as indicated on the panels.

sager type, it is predicted that when the energy of the absorption of an allowed electronic transition is plotted vs. $(n_D^2 - 1)/(2n_D^2 + 1)$, a straight line should be obtained, the slope of which is a function of the oscillator strength of the transition and the Onsager radii of the solute, while its intersection with the energy axis gives the origin of the absorption in the gas phase, ν_{gas}. In Fig. 3 such plots are shown for DPH and its two derivatives. The ν_{sol} energy for the various hexane/benzene mixtures was that of the O–O vibrational peak of the absorption and it was obtained by analysing the absorption spectra in terms

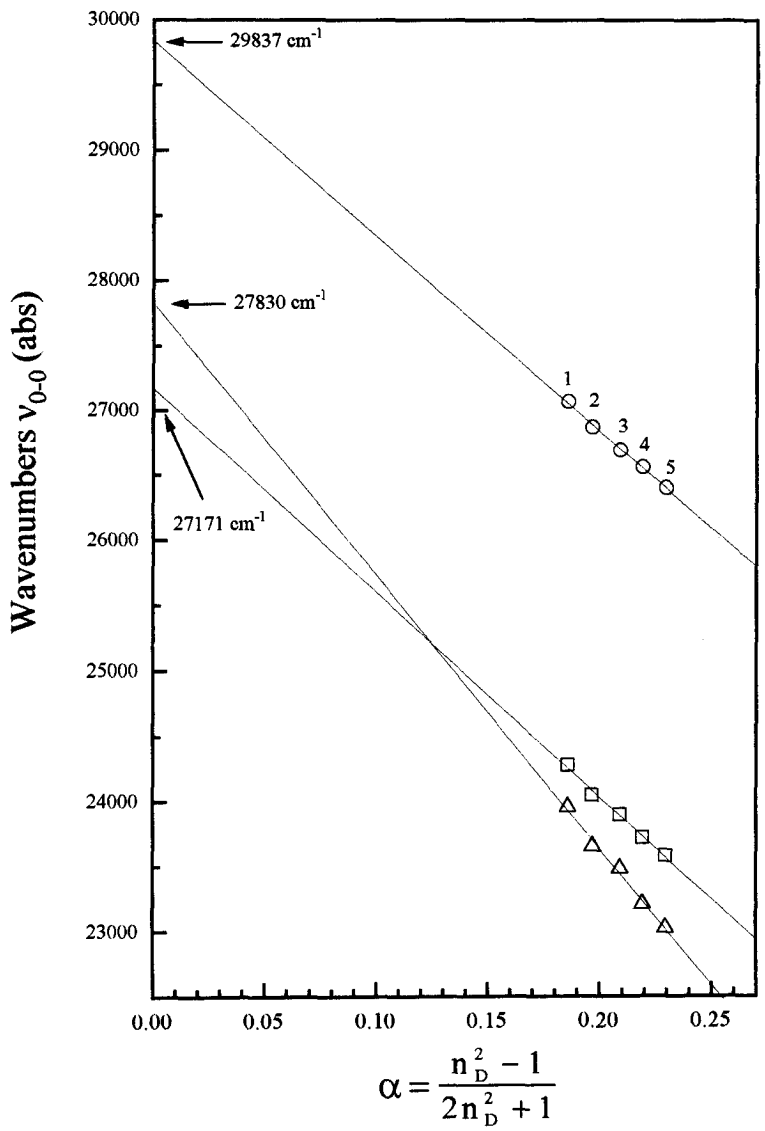

Fig. 3. Plots of the energies of the O–O absorption in solution, ν_{sol}, vs. electron polarizability $\alpha = (n_D^2 - 1)/(2n_D^2 + 1)$ for hexane–benzene mixed solvents. (○) DPH; (□) DPH–$N(CH_3)_2$; (△) DPH–NO_2. (1) hexane; (2) hexane/benzene = 3/1; (3) 1/1; (4) 1/3; (5) benzene.

of gaussian curves. These plots produce straight lines for all three molecules, including the polar derivatives, whereas extrapolations to $n_D = 1$ give the origin of the corresponding absorptions in the gas phase, viz. 29837 cm^{-1} for DPH, 27830 cm^{-1} for DPH–NO_2 and 27171 cm^{-1} for DPH–$N(CH_3)_2$. This ν_{gas} value for DPH is very close to the ν_{gas} values reported in the literature for diphenylpolyenes [23], whereas although numbers are not available for the two polar derivatives, the values found here appear very reasonable. Note, also that the slope of the straight lines obtained from fitting the absorption data are very similar for DPH and its two derivatives, in agreement with the strong oscillator strength that all these molecules possess, and their similar molecular sizes which indicate similar Onsager radii for all three of them.

3.2. Fluorescence

Although the solvent effects on the absorption spectra are essentially similar in DPH and in the two derivatives, large and important spectroscopic differences are observed in the corresponding fluorescence spectra. Thus, examination of Figs. 1, 2 and 4 shows that the emission of DPH is totally insensitive to the nature of the solvent, it exhibits a large apparent Stokes shift, close to 3000 cm^{-1}, and there is no mirror image between the absorption and fluorescence spectra. All these are characteristic signs of a forbidden transition, such as the $^1A_g(S_0) \leftarrow {}^1A_g(S_1)$ which has been shown to account for the intense emission of DPH [24]. Note, however that the weak high energy fluorescence (h.e.f.) at ca. 26000 cm^{-1}, changes its position in the various solvents (see Fig. 4a), has ordinary Stokes shift and it exhibits mirror image symmetry with the absorption spectrum, (barely discernible in Fig. 1a, see however Ref. [24]), in accordance with the allowed character of the corresponding transition $^1A_g(S_0) \leftarrow {}^1B_u(S_2)$ [24]. The emission of the derivatives on the contrary, demonstrates a totally different behaviour. Their fluorescence spectra are strongly dependent on the solvent. Thus, in solvents with high dielectric constant, such as acetonitrile and DMF the fluorescence red shifts are exceptionally large as shown in Figs. 2b and 4b–c, e.g., the spectral shift of DPH–NO_2, upon change of the solvent from hexane to acetonitrile is as large as 7000 cm^{-1} (see Fig. 4c). It must be pointed out however, that such large stabilizations of the emitting states, is rather difficult to be attributed exclusively to solvent relaxation processes. Instead, some state-mixing, or perhaps formation of charge transfer emitting states, may be contributing towards these unusually large fluorescence red shifts. In any case, the very high sensitivity of the emission of these DPH derivatives to the 'polarity' of the environment is what makes them ideally suited for fluorescence probing studies. The absorption and fluorescence spectra of DPH and of the two derivatives in various solvents, shown in Figs. 1 and 2, demonstrate different behaviour as far as the vibrational structure of the spectra is concerned. Thus, the polar solutes DPH–$N(CH_3)_2$ and DPH–NO_2 when in polar solvents exhibit blurred spectra with imperceptible vibrational structure. On the other hand, the apolar DPH in all solvents and the polar derivatives in the apolar solvent hexane demonstrate discernible vibrational structure. This is due to the strong dipole–dipole interactions which broaden the energies of the individual vibrational states resulting to mutual overlap and obliteration of the vibrational spectral structure when polar chromophores are dissolved in polar solvents.

It is interesting to note that the nitro derivative does not emit when dissolved in alcoholic media. To study this peculiarity we have measured the fluorescence lifetime τ(exp) of a 1.25×10^{-6} M solution of DPH–NO_2 in *p*-dioxane and in three other solutions prepared by the separate addition to the previous solution of 0.68 M, of methanol, of ethanol and of ethylene glycol. In these three solutions τ(exp) was found to be equal to that in the solution of pure *p*-dioxane, viz. 1.48 ns, indicating that the fluorescence quenching is caused by a ground state complex formed between DPH–NO_2 and the added alcohol. To determine the strength of these complexes, we performed a Stern–Volmer type titration on the DPH–NO_2 in *p*-dioxane, using methanol, ethanol and ethylene glycol as the quencher. The association constants thus obtained were 8.6×10^{-2} M^{-1} for methanol, 3×10^{-2} M^{-1} for ethanol and 1.25 M^{-1} for ethylene glycol. These numbers are in agreement with the increasing hydrogen bonding ability in the order ethanol, methanol, ethylene glycol, therefore we have concluded that ground state H-bonding is

responsible for the lack of fluorescence from DPH–NO_2 in alcohols.

Among the various theories which have been proposed to account for the so-called solvatochromic shift, defined as the difference $\nu(\text{abs})_{max} - \nu(\text{fluo})_{max}$, between the absorption and fluorescence

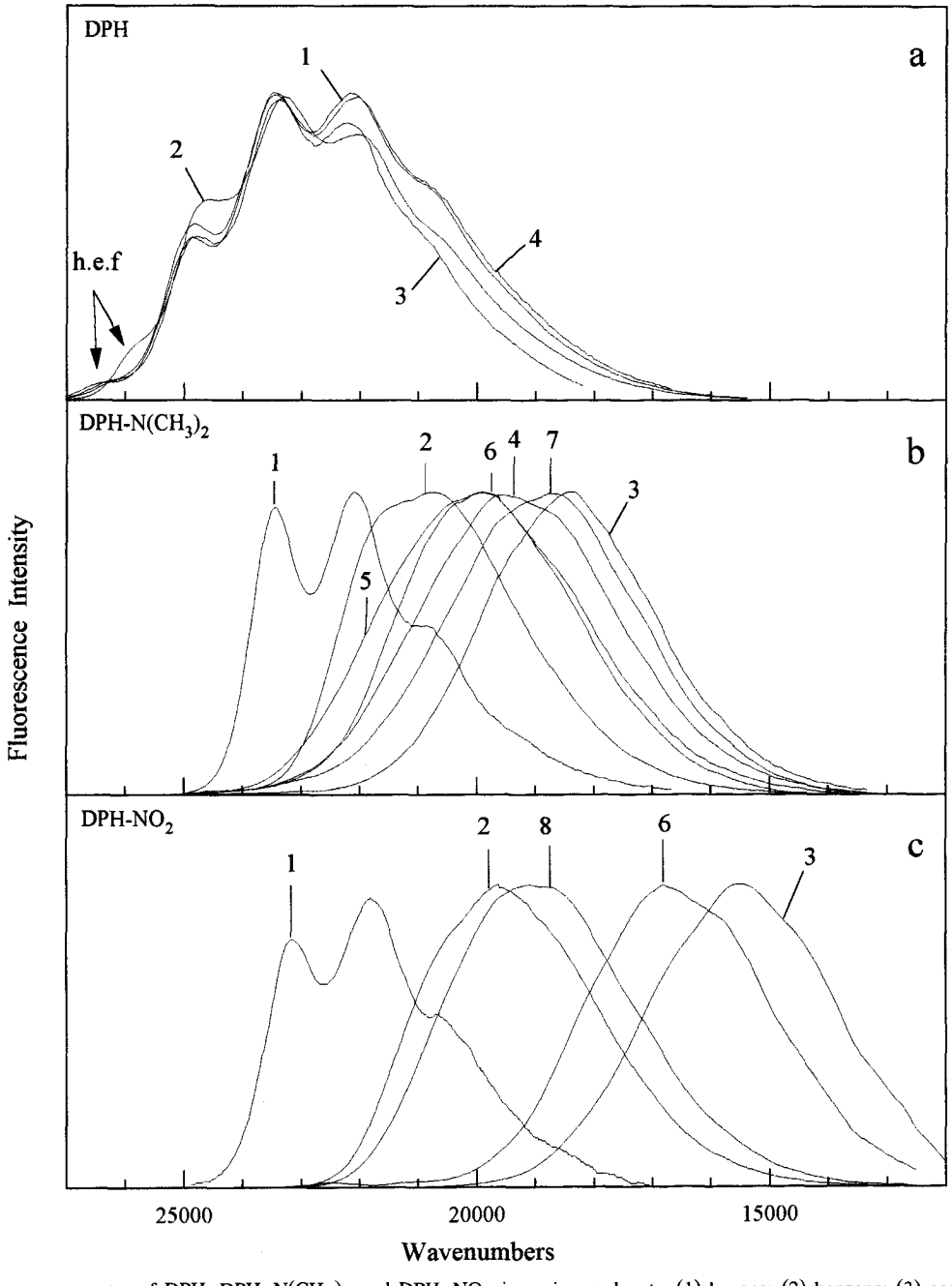

Fig. 4. Fluorescence spectra of DPH, DPH–$N(CH_3)_2$ and DPH–NO_2 in various solvents. (1) hexane; (2) benzene; (3) acetonitrile; (4) ethanol; (5) butanol; (6) chloroform; (7) methanol; (8) *p*-dioxane.

maxima, the one by Lippert [25] is the simplest and also the most widely employed. The theory ignores any specific solvent–solute interactions and deals only with the general solvent effects, which are the result of dielectric interactions, viz. multiple moments and polarizability properties of solute and solvent molecules, described collectively as 'solvent polarity'. The important solvent parameter is the orientation polarizability Δ_f, expressed in terms of the dielectric constant and the refractive index of the medium as Eq. (1)

$$\Delta_f = (\epsilon - 1)/(2\epsilon + 1) - (n_D^2 - 1)/(2n_D^2 + 1) \quad (3)$$

The theory predicts that the solvatochromic shift (SS) between the absorption and fluorescence maxima, is to a good approximation,

$$\mathrm{SS}\ (\mathrm{cm}^{-1}) \approx \frac{2\Delta_f(\mu_{exc} - \mu_{gr})^2}{\hbar c R^3} + C \quad (4)$$

In Eq. (4), $\hbar$ and c are the Planck constant and the velocity of light, μ_{exc} and μ_{gr} are the dipole moments of the solute in the excited and ground state, R is the radius of the Onsager cavity of the solute and C is a constant. Plots of SS vs. Δ_f are shown in Fig. 5 for DPH and derivatives II and III. Considering the very approximate nature of the Lippert equation, the agreement between theory and experiment is quite satisfactory. From the slope of the straight lines the increase of the dipole moment of the two

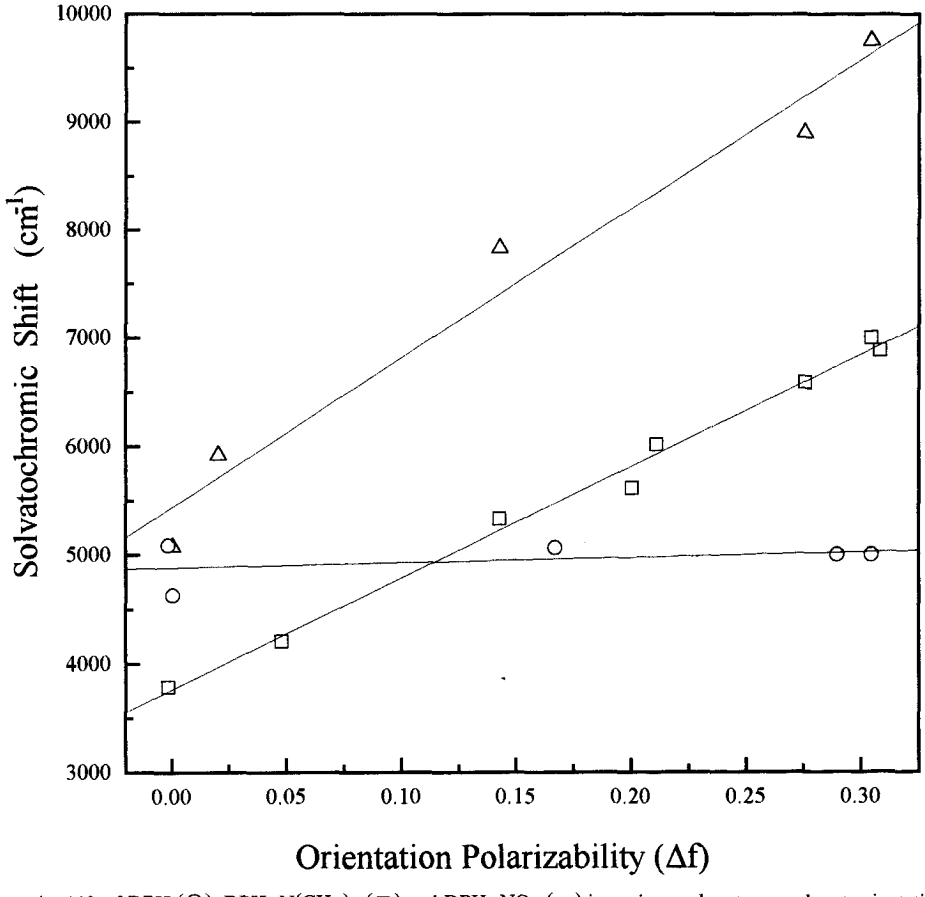

Fig. 5. Solvatochromic shift of DPH (○), DPH–N(CH$_3$)$_2$ (□) and DPH–NO$_2$ (△) in various solvents vs. solvent orientation polarizability $\Delta_f = (\epsilon - 1)/2\epsilon + 1) - (n_D^2 - 1)/(2n_D^2 + 1)$.

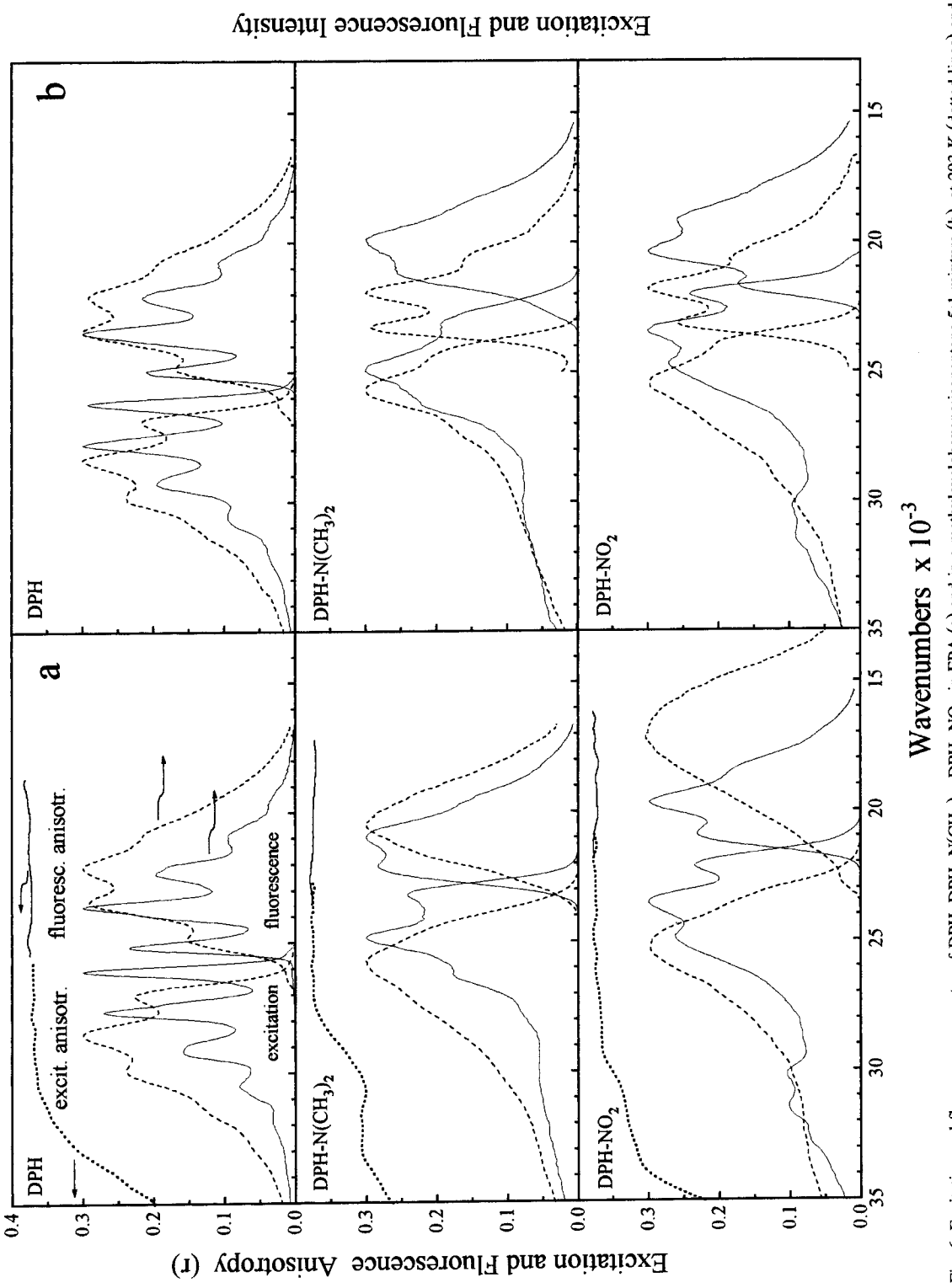

Fig. 6. Excitation and fluorescence spectra of DPH, DPH–$N(CH_3)_2$, DPH–NO_2 in EPA (a) and in a methylcyclohexane:isopentane 5:1 mixture (b), at 293 K (dotted lines) and 77 K (solid lines). Excitation (solid lines) and fluorescence (dashed lines) anisotropies are also shown for EPA (a), they are the same for methylcyclohaxane–isopentane mixture.

molecules upon excitation can be estimated, thus we found $\mu_{exc} - \mu_{gr} = 7D$ and 10D for the dimethylamino and the nitro derivative, respectively. Interestingly enough, although the Lippert equation is valid only for protic solvents, the experimental points of DPH–$N(CH_3)_2$ dissolved in alcohols, lie nevertheless on the same straight line as the other points corresponding to aprotic solvents. Note, that the widely employed biological fluorescence probe prodan, in a similar plot exhibits two differently disposed straight lines, one for protic and another for aprotic solvents [26]. Finally it should be noted that while alcohols quench the emission of DPH–NO_2, they do not seem to affect much the fluorescence of DPH–$N(CH_3)_2$.

The fluorescence behaviour of the derivative molecules differs from that of DPH also with regard to the Stokes shift. This shift is ca. 900 cm^{-1} in II and III dissolved in the inert solvent hexane, compared with the ca. 3000 cm^{-1} measured in DPH (Fig. 1a). At liquid nitrogen temperature the Stokes shift becomes less than 250 cm^{-1} for the derivatives in an aliphatic glass, while is still large for DPH (Fig. 6b). Other equally important difference in the emission spectra of the amino and nitro molecules on the one hand and DPH on the other is the absorption–fluorescence mirror image relationship, which is demonstrated by the derivatives but not by DPH. This mirror image symmetry was shown to hold in the case of the derivatives by deconvoluting the spectra using gaussian type functions. For instance, in the case of DPH–NO_2 in hexane (Fig. 1a), the spacings between the first three absorption peaks were found equal to 1289 and 1272 cm^{-1}, while the corresponding energies in fluorescence were 1287 and 1300 cm^{-1}. Similarly, the heights of the corresponding absorption–emission peaks were closely equal, in agreement with the mirror image relationship. Beyond the third absorption peak there is interference from the next electronic transition and it is difficult to extract the spacings between the higher energy peaks as well as their relative heights.

3.3. Temperature effect

The effect of temperature on the fluorescence is nearly zero in DPH but very important in the derivatives. This is shown in Fig. 6 where absorption–fluorescence spectra of the three molecules in the apolar mixture 5:1 methylcyclohexane:isopentane, and the partially polar EPA (5:5:2, isopentane:ethylether:ethanol) at 293 K and at liquid nitrogen temperature are reproduced. At lower temperature the absorption spectra of all three molecules, in both polar and apolar solvents, demonstrate a red shift with respect to the room temperature spectra. This stabilization of the excited Franck–Condon states is attributed to the increase of the solvent refractive index occurring at lower temperature, and the ensuing increased electron polarizability of the solvent molecules. Evidently, this shift is larger when the solute is polar and possesses permanent dipole moment in the excited state than when it is apolar. This behaviour is clearly exhibited by the absorption spectra of Fig. 6. In contrast, in the low temperature fluorescence spectra, the situation is different between polar and apolar solvents. Thus, when the solvent is apolar the excited state stabilization depends only on refractive index, and therefore increases with decreasing temperature, resulting to fluorescence red shift with respect to the high temperature spectrum. This is evident in the fluorescence spectra of the derivatives dissolved in the apolar methylcyclohexane:isopentane mixture (Fig. 6b). However, when the solvent is polar it stabilizes the excited state not only on account of its refractive index but also by means of the reorientation of its molecules due to interactions of their permanent dipoles with the solute dipole moment. At low temperatures, though, when the solvent is frozen, reorientation is not possible and therefore the stabilization of the excited state is less than at room temperature. Consequently, the fluorescence spectra are expected to shift to the blue when the temperature is lowered from 293 to 77 K, exactly as shown in Fig. 6a. Note, that the fluorescence of DPH is temperature independent because of the already mentioned forbidden character of the corresponding transition. Clearly, all the above differences in the emission behaviour of DPH and its two derivatives, viz. solvent and temperature dependence, Stokes shift and absorption–fluorescence mirror image symmetry, point to the conclusion that, contrary to what happens in DPH, the fluorescence of DPH–$N(CH_3)_2$ and DPH–NO_2 originates from the same excited state which was

Table 1
Fluorescence parameters of I, II, III in various solvents

Solvent	ϵ	n_D	Φ_f			τ(exp)[a]			τ(rad)[a]			τ(intr)[a]			r[b]	
			DPH	-amino	-nitro	DPH	-amino	-nitro	DPH	-amino	-nitro	DPH	-amino	-nitro	-amino	-nitro
Hexane	1.88	1.372	0.63	0.265	≈ 0.002	15.9	0.50	0.126 (2.4)[c]	25.2	1.89	42–126[d]	2.39	2.68	3.5	0.037	0.27
p-Dioxane	2.21	1.422	0.80	0.12	0.46	9.2	0.23	1.48	11.5	1.9	3.2	2.25	3.44	5.26	0.171	0.045
Benzene	2.28	1.498	0.76	0.12	0.396	7.0	0.23	1.03	9.2	1.9	2.6	1.6	3.37	4.98	0.126	0.030
$CHCl_3$	4.64	1.444	0.57	0.063	0.35	6.2	0.176 (0.8)[e]	2.1	10.9	2.8	6	2.7	3.8	7.98	0.152	0.024
ETOH	24.3	1.359	0.26	0.037	–[f]	6.65 (5.6)[g]	0.141 (0.57)[e]	–	25.6	3.8	–	2.38	4.13	–	0.214	–
MeOH	32.6	1.326	0.23	0.029	–	4.8	0.121 (0.41)[e]	–	20.9	4.17	–	2.3	4.37	–	0.207	–
CH_3CN	36.2	1.342	0.17	0.034	0.140	4.01	0.144 (0.34)[e]	1.3 (1.5)[c]	23.6	4.2	9.3	2.7	4.69	9.8	0.145	0.02
DMF	37	1.427	0.35	0.054	0.22	3.4	0.20	1.84	9.7	3.7	8.36	1.5	3.9	9.7	0.171	0.03
Ethyl ether	4.33	1.352	0.74	0.053	0.25	15.2	0.19	0.82	20.5	3.58	3.3	2.5	3.8	4.1	0.128	0.012

ϵ, dielectric constant. n_D, refractive index.
[a] Fluorescence lifetimes expressed in ns.
[b] All r values of DPH were below 0.01 due to its high τ(exp).
[c] Different τ(exp) reported in Ref. [8].
[d] Due to the uncertainty of the magnitude of the quantum yield τ(rad) varies within a large range.
[e] Different τ(exp) reported in Ref. [10].
[f] Non-fluorescent.
[g] Different τ(exp) reported in Ref. [7].

created by the absorption of light, and which has an allowed transition moment to the ground state.

3.4. Fluorescence quantum yields

The fluorescence quantum yields of I, II and III in various solvents are listed in Table 1. From these data it becomes evident, that Φ_f exhibits a general tendency to decrease as the dielectric constant of the solvent increases, and also that DPH has a higher quantum yield than its two derivatives in all solvents. Both these trends can be rationalized in terms of the increasing solute–solvent interactions as ϵ increases, particularly when the solute is polar, like the two derivatives of DPH. These increased interactions result to stabilization of the emitting state, i.e., decrease of the S_1–S_0 energy gap, as clearly demonstrate by the red shifts of the corresponding fluorescence spectra in Figs. 1, 2 and 4. This decrease of the energy gap between the first excited singlet and the ground state increases the probability for radiationless deactivation, and explains the decrease of Φ_f with increasing ϵ. Moreover, the stabilization of the S_1 state is larger in the polar derivatives, due to the stronger solute–solvent interactions, than in the apolar DPH, and this is the reason for the higher Φ_f values in DPH than in the derivatives. There is however an exception to the general tendency of decreasing Φ_f with increasing ϵ. This is the case of DPH–NO_2 in hexane which has an extremely low quantum yield equal to $2 \times 10^{-3} \pm 1 \times 10^{-3}$.

The feeble fluorescence of DPH–NO_2 when it is dissolved in aliphatic environment (hexane and other alkanes) was studied as a function of temperature between 293 and 77 K. For an assumed number of n temperature dependent radiationless deactivation paths of the first excited singlet state, the well-known Arrhenius type equation [27]

$$\ln\frac{1-\Phi_f}{\Phi_f} = \sum_n \left(\ln\frac{A_n}{k_f} - \frac{E_n}{RT}\right) \tag{5}$$

holds, where $k_f = \Phi_f/\tau(\exp)$ is the fluorescence rate constant, assumed to be temperature independent, E_n is the energy barrier for the nth radiationless path, and A_n, R, T are the usual parameters of the Arrhenius equation. In accordance with this equation, we have measured the temperature dependence of the

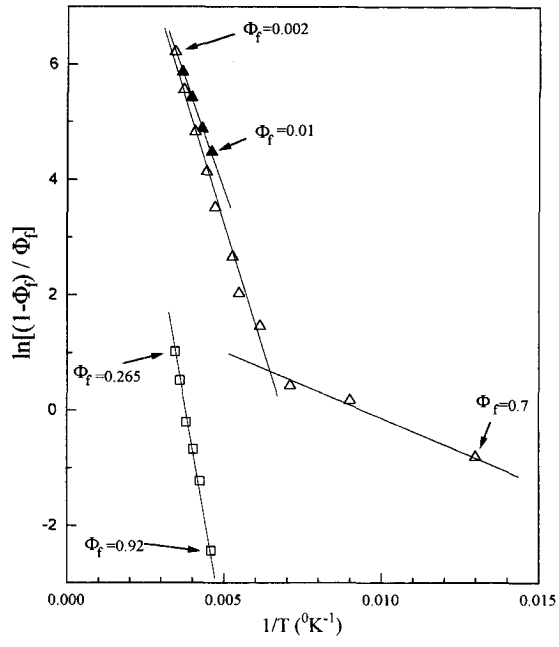

Fig. 7. Arrhenius plot of the temperature dependence of the fluorescence quantum yield for DPH–$N(CH_3)_2$ (□) and DPH–NO_2 (△).

quantum yield of DPH–NO_2 in hexane in the range 293 to 220 K, and for comparison, we have also measured the Φ_f of DPH–$N(CH_3)_2$, which does not present the problem of the very low quantum yield in hexane. The results are shown in Fig. 7 and they indicate that the activation energy barrier for the radiationless transition is ca. 2.9 kcal/M in the case of the nitro and 5.8 kcal/M in the amino derivative. Both these values fall within the range of activation energies reported in the literature for *cis–trans* isomerization of similar molecules [28]. However, the important point is that although the relative fluorescence quantum yield of the nitro derivative increases by approximately 10-fold when the temperature is lowered down to 220 K, the absolute value of Φ_f remains very low, it does not exceed 0.015, while the corresponding Φ_f of the amino derivative becomes as high as 0.92 at 220 K. Evidently, there must be an additional deactivation path (or paths) which accounts for the observed large loss of excitation in DPH–NO_2/hexane. To search for the fate of the excitation in DPH–NO_2 we have looked at even lower temperatures using the glass forming mixture

of methylcyclohexane:isopentane 5:1, in which the quantum yield of DPH–NO_2 at room temperature is as low as it is in hexane. The new data, also plotted in Fig. 7, show that the high temperature barrier in this solvent is 3.6 kcal/M, i.e., about the same as in hexane, whereas below ca. 120°K another energy barrier enters the picture, with considerably lower energy, $E = 0.43$ kcal/M, and therefore less pronounced temperature dependence, than the previous barrier. Extrapolation of the Arrhenius plot to the limit $\Phi_f = 1$, and assuming that no additional processes of radiationless decay appear below 120 K, shows that at ca. 32 K the quantum yield will become equal to one. Note that the corresponding temperature for the amino derivative, estimated from a similar extrapolation of its plot in Fig. 7, is ca. 208 K.

3.5. Effect of viscosity

The evidence that the low fluorescence quantum yield in alkanes may be related to *trans–cis* photoisomerization, has suggested the study of the effect of the viscosity of the medium on Φ_f. We have measured the quantum yield of DPH and of its two derivatives, in hexane–nujol mixtures of varying composition from 100% hexane to 100% nujol, having viscosity varying from 0.3 to 120 cP. The results are depicted in Fig. 8 in terms of the ratio of the values of Φ_f in the mixture and in pure hexane, $\Phi_f(\text{mix})/\Phi_f(\text{hex})$, vs. the vol% of nujol in the mixture. In DPH this ratio is practically independent of viscosity, but in the derivatives it increases with viscosity, the increase being much larger in the nitro derivative. This different rise of Φ_f with viscosity in

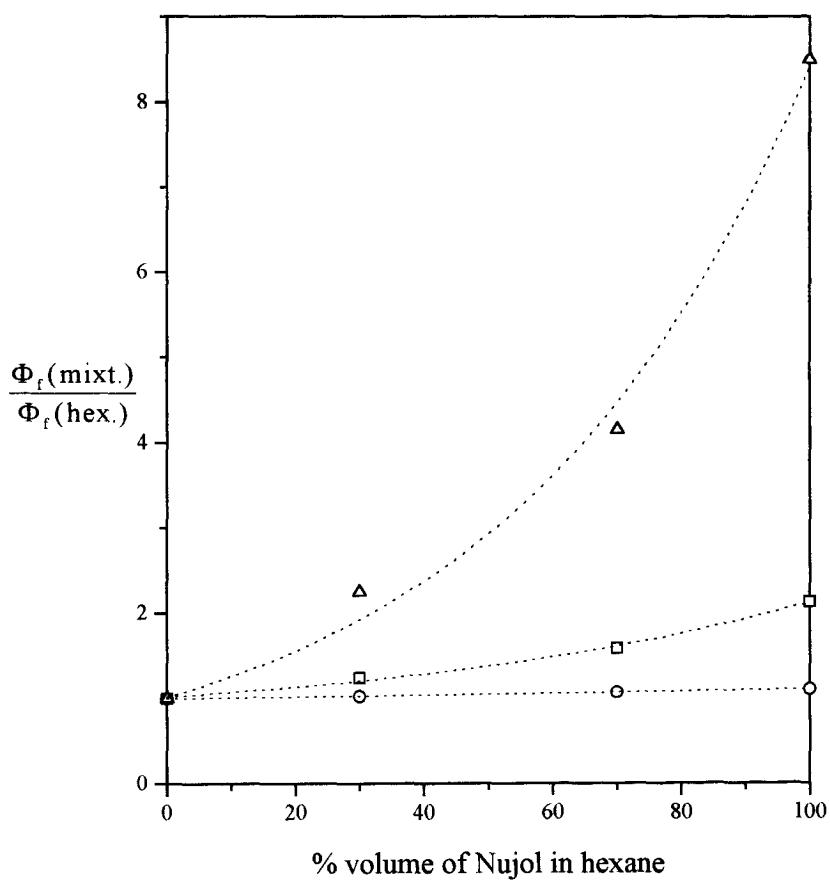

Fig. 8. Plot of the ratio of the fluorescence quantum yield in the nujol–hexane mixture over the quantum yield in pure hexane vs. vol% of nujol in hexane. (○) DPH; (□) DPH–$N(CH_3)_2$; (△) DPH–NO_2.

the two derivatives is in good qualitative agreement with the higher activation energy derived from the Arrhenius plot of Fig. 7, for the presumed *trans–cis* isomerization, viz. $E_{amino} = 5.8$ kcal/M and $E_{nitro} = 2.9$ kcal/M). In other solvents than alkanes, it is difficult to discuss the effect of the viscosity on Φ_f, because other parameters, e.g., dielectric constant, the refractive index, the hydrogen bonding ability of the solvent etc, affect the measurement of the quantum yield. However, data from the literature [18] for the quantum yield of DPH in alcohols of different viscosity, show a lesser variation of Φ_f, than in the amino derivative, e.g., our measurements have shown that the Φ_f of DPH–N$(CH_3)_2$ rises from ca. 0.029, when the solvent is methanol (viscosity 0.5) to 0.037 in ethanol (visc. 1.2) to 0.1 in ethylene glycol (visc. 20), whereas the Φ_f of DPH goes from 0.23 in methanol only up to 0.37 in *n*-butanol (visc. 2.95). The nitro derivative does not fluoresce in alcohols.

3.6. Fluorescence lifetimes

The experimental fluorescence lifetimes, listed in Table 1, show the same trend with that of Φ_f, thus τ(exp) decreases as ϵ increases, with the exception of DPH–NO_2 in hexane which again behaves differently. The origin of this trend is the same as that of the variation of Φ_f with ϵ, viz. energy stabilization of the emitting state due to the increased solute–solvent interactions. The radiative fluorescence lifetime τ(rad), being the ratio of the two similarly varying parameters, Φ_f and τ(exp), shows a rather small variation for the same solute in the different solvents, with the exception of DPH–NO_2 in hex-

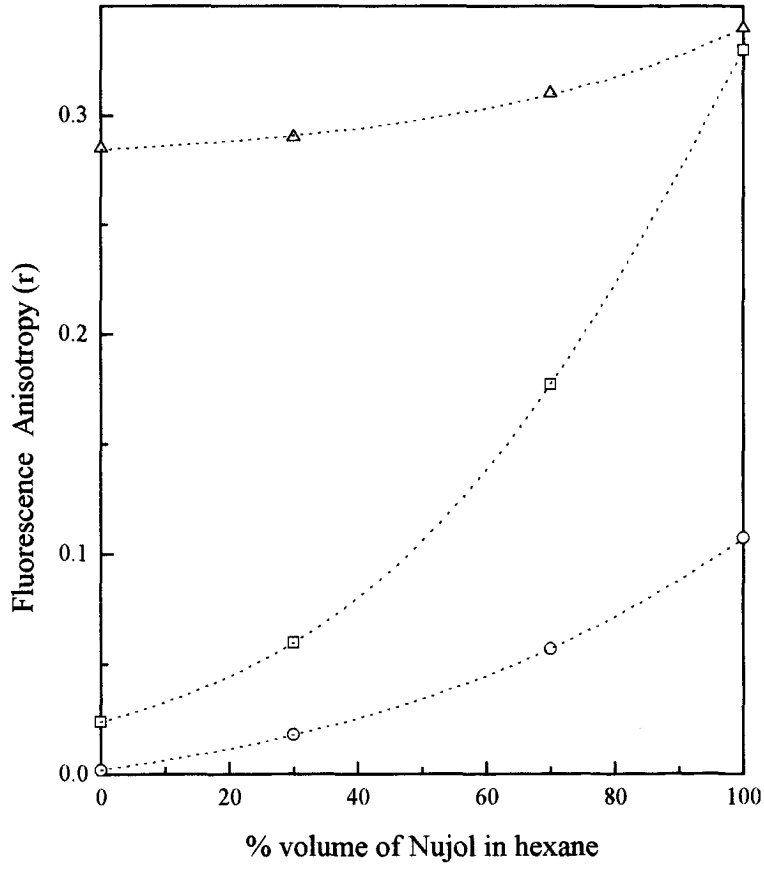

Fig. 9. Plot of fluorescence anisotropy (r) vs. vol% of nujol in hexane. (○) DPH; (□) DPH–N$(CH_3)_2$; (△) DPH–NO_2.

ane. τ(rad) is however, quite larger in the parent molecule DPH than in the derivatives, particularly the DPH–N$(CH_3)_2$. Finally, the intrinsic fluorescence lifetimes τ(intr), determined from the absorption spectra [17], are very much the same, within a factor of less than 2, for each one of the three polyenes in all solvents. An important parameter however is the ratio $\tau(\text{rad})/\tau(\text{intr})$, which is close to one for the two derivatives (within a factor of 2), but it is as large as 10 in DPH. This discrepancy between the parent molecule and its derivatives is attributed to the different nature of the emitting state in the two cases. In DPH the fluorescence is symmetry forbidden, whereas in the derivatives it is allowed and therefore τ(rad) is ordinarily expected to be approximately equal to τ(intr). The magnitude of the experimental fluorescence lifetime τ(exp), on the other hand, in association with the viscosity of the medium, is the determining factor for the value of the fluorescence anisotropy r, and therefore it influences the application of these molecules as fluidity probes.

3.7. Fluorescence anisotropy

The fluorescence anisotropy is defined as $r = (I_{VV} - GI_{VH})/(I_{VV} + 2GI_{VH})$, where I stands for the fluorescence intensity and the subscripts describe the vertical or horizontal settings of the excitation and fluorescence polarizers. The factor $G = I_{HV}/I_{HH}$ compensates for any differences in the instrument response between vertically and horizontally polarized light [29]. The maximum possible r values, $r_{max} = r_0$, were measured in vitrified solutions, viz. glycol at 220 K and in EPA and methylcyclohexane:isopentane 5:1, at 77 K, to prevent any rotation of the fluorophor. We found $r_0 = 0.38$ for all three molecules. Note, that the r_0 values reported in the literature for DPH range between 0.36 and 0.39 [30,31]. As is seen in Fig. 6, the value $r_0 = 0.38$ is constant at all wavelengths above 360 nm (below ca. 28 000 cm^{-1}), i.e., across the entire range of the lowest electronic transition. The maximum possible value of r_0, when the absorption and fluorescence transition moments are exactly parallel is $r_0 = 0.4$, the values found here, viz. $r_0 = 0.38$, indicate that the absorbing and emitting transition moments deviate by approximately 10° from being parallel to each other. it is interesting, that although in DPH two different states are involved in absorption and emission, viz. the ^1B_u and the ^1A_g, respectively, whereas in the derivatives the same state absorbs and emits, still in both cases emission and absorption transition moments deviate by the same angle of ca. 10°. The room temperature r values of the two derivatives are listed in Table 1 for solvents ranging in viscosity from ca. 0.3 to 1.2 cP. DPH is not included in this list because its r values are very low, less than 0.01, in all solvents with common viscosities, and therefore r cannot be determined with accuracy. The reason for this is that DPH has very long τ(exp) compared with its rotational correlation time, τ(corr), in non-viscous media [32]. Thus, from the Einstein equation, $\tau(\text{corr}) = \eta V/RT$, where η is the viscosity of the solvent, V the molecular volume of the fluorophore, R the gas constant and T the absolute temperature, τ(corr) for DPH in hexane is estimated to be ca. 0.025 ns at room temperature (molecular volume of DPH = 207.4 cm^3) [33]. The corresponding fluorescence lifetime, on the other hand, is many times longer, τ(exp) = 15.9 ns, therefore DPH has enough time to tumble many times before it emits, resulting in the total randomization of its fluorescence anisotropy. The derivatives, on the contrary, and in particular DPH–N$(CH_3)_2$, which have similar τ(corr) with DPH, have nevertheless much shorter fluorescence lifetimes (Table 1), therefore their r values are rather sensitive to the viscosity of the environment. The dependence of r on the viscosity of the environment —expressed in terms of the composition of a hexane–nujol mixture— is shown in Fig. 9 for I, II and III. It is seen that the fluorescence anisotropy of DPH–N$(CH_3)_2$ in an aliphatic environment, is more sensitive to the viscosity than the r of the two other homologues.

4. Conclusions

The main conclusions of the present study can be summarized as follows. (1) In Contrast to the parent molecule DPH, the absorption and emission in the derivatives involve the same excited state, with the corresponding transitions allowed. (2) The fluorescence quantum yields decrease with increasing solvent polarity, except the nitro derivative in hexane which shows anomalous behaviour due to a small

energy barrier of a radiationless deactivation path. The same trend is exhibited by the lifetimes, τ(exp). (3) The viscosity of the environment has a sizable effect on the quantum yields of the derivatives (more pronounced in DPH–$N(CH_3)_2$), but nearly non in DPH. (4) Because of differences in fluorescence lifetimes τ(exp), the fluorescence anisotropy is strongly dependent on the viscosity in DPH–$N(CH_3)_2$ but less so in DPH and the nitro derivative. (5) Finally, the two derivatives prove to be excellent fluorescent probes, as concluded by the fact that their emission spectra show great dependence on the solvent polarity, whereas their fluorescence anisotropy depends on the viscosity of the medium.

References

[1] B.S. Hudson, B.E. Kohler, J. Chem. Phys. 59 (1973) 4984.
[2] J. Saltiel, D.-H. Ko, S.A. Fleming, J. Am. Chem. Soc. 116 (1994) 4099.
[3] B.S. Hudson, B.E. Kohler, Chem. Phys. Lett. 14 (1972) 299.
[4] K. Schulten, M. Karplus, Chem. Phys. Lett. 14 (1972) 305.
[5] B.E. Kohler, Chem. Rev. 93 (1993) 41, and references cited therein.
[6] B.R. Lenz, Chem. Phys. Lipids 50 (1989) 171.
[7] E.D. Cehelnik, R.B. Cundall, J.R. Lockwood, T.F. Palmer, J. Phys. Chem. 79 (1975) 1369.
[8] R.B. Cundal, I. Johnson, M.W. Jones, E.W. Thomas, Chem. Phys. Lett. 64 (1979) 39.
[9] P.J. Trotter, J. Storch, Biochim. Biophys. Acta 982 (1989) 131.
[10] F.G. Prendergast, R.P. Haugland, P.J. Callahan, Biochemistry 20 (1981) 7333.
[11] M.T. Allen, L. Miola, D.G. Whitten, J. Am. Chem. Soc. 110 (1988) 3198.
[12] P.C. Alford, T.F. Palmer, J. Chem. Soc. Faraday Trans. 79 (1983) 433.
[13] P.C. Alford, T.F. Palmer, Chem. Phys. Lett. 86 (1982) 248.
[14] G. Pistolis, A. Malliaris, Langmuir 13 (1997) 1457.
[15] B.E. Kohler, J. Chem. Phys. 93 (1990) 5838.
[16] J.N. Demas, G.A. Crosby, J. Chem. Phys. 75 (1971) 991.
[17] J.B. Birks, D.J. Dyson, Proc. R. Soc. A 275 (1963) 135.
[18] S.L. Bondarev, S.M. Bachilo, J. Photochem. Photobiol. A: Chem. 59 (1991) 273.
[19] S. Basu, Adv. Quant. Chem. 1 (1964) 145.
[20] N. S Bayliss, J. Chem. Phys. 18 (1950) 292.
[21] N.S. Bayliss, E.G. McRae, J. Phys. Chem. 58 (1954) 1002.
[22] N.S. Bayliss, E.G. McRae, J. Phys. Chem. 58 (1954) 1006.
[23] K.W. Hausser, R. Kuhn, A. Smakula, K.H. Kreuchen, Z. Phys. Chem. B29 (1935) 363.
[24] B. E Kohler, T. Itoh, J. Phys. Chem. 92 (1988) 5120.
[25] E. Lippert, Z. Electrochem. 61 (1957) 962.
[26] G. Weber, F.J. Farris, Biochemistry 18 (1979) 3075.
[27] M.N. Pisanias, D. Schulte-Frohlinde, Ber. Bunsen-Gesellschaft 79 (1975) 662.
[28] S.P. Velsko, G.R. Fleming, J. Chem. Phys. 76 (1982) 3553.
[29] P.O. Anderson, S.M. Bachilo, R.-L. Chen, T. Gilbro, J. Phys. Chem. 99 (1995) 16199.
[30] M. Shinitzky, Y. Barenholz, Biochem. Biophys. Acta 515 (1987) 367.
[31] C.R. Mateo, M.P. Lillo, J.C. Brochon, M. Martinez-Ripoll, J. Sanz-Aparicio, A.U. Acuna, J. Phys. Chem. 97 (1993) 3486.
[32] J.R. Lakowicz, Principles of Fluorescence Spectroscopy, Plenum Press, New York, 1983, p. 135.
[33] T. Hall, M. Bachrach, C.W. Spangler, L.S. Sapochak, C.T. Lin, H.W. Guan, R.D. Rogers, Acta Cryst. C 45 (1989) 1541.